

# Deep learning for COVID-19 diagnosis based feature selection using binary differential evolution algorithm

Mohammad Saber Iraji <sup>a,c</sup>, Mohammad-Reza Feizi-Derakhshi <sup>b,\*</sup>, Jafar Tanha <sup>c</sup>

<sup>a</sup> *Department of Computer Engineering and Information Technology, Payame Noor University, Tehran, Iran*

<sup>b</sup> *Computerized Intelligence Systems Laboratory, Department of Computer Engineering, University of Tabriz,  
Tabriz, Iran*

<sup>c</sup> *Faculty of Electrical and Computer Engineering, University of Tabriz, Tabriz, Iran*

*Corresponding author: Mohammad-Reza Feizi-Derakhshi (mfeizi@tabrizu.ac.ir)*

## **Abstract**

The new Coronavirus is spreading rapidly and it has taken the lives of many people so far. The virus has destructive effects on the human lung and early detection is very important. Deep Convolution neural networks are a powerful tool in classifying images. Therefore, in this paper a hybrid approach based on a deep network is presented. Feature vectors were extracted by applying a deep convolution neural network on the images and effective features were selected by the binary differential meta-heuristic algorithm. These optimized features were given to the SVM classifier. A database consisting of three categories of images as COVID-19, pneumonia, and healthy included 1092 X-ray samples was considered. The proposed method achieved an accuracy of 99.43%, a sensitivity of 99.16%, and a specificity of 99.57%. Our results demonstrate the suggested approach is better than recent studies on COVID-19 detection with X-ray images.

**Keywords**— Deep convolution, COVID-19, Meta-heuristic, Binary differential, Neural networks, X-ray image

## 1. INTRODUCTION

The rapid spread of COVID-19 has killed many people around the world. The disease is associated with symptoms such as muscle aches, coughs, fevers, and can be detected through clinical trials and radiographic imaging. Medical imaging is very important in diagnosing diseases. The X-rays and computed tomography (CT) scans of the disease can be used in the deep network to help diagnose the disease more quickly.

The process of classifying and diagnosing the disease from a photo using a neural network consists of 4 main steps: feature extraction, optimal feature selection, network training, and model performance test. Feature extraction is of two types. In the first case: The extraction of features from images include the shape of tissues and texture for patient classification is done using image processing techniques, algorithms, and filters. In the second type, the original images and their actual output class were entered into the convolution network as input data, and after the network training process and weight adjustment, the features were automatically extracted in the last full layer.

Some features extracted from the deep network may have a detrimental effect on the accuracy of the classification [1]. Therefore, the optimal feature selection methods are essential. There are three types of feature selection methods. The filter method, which uses the intrinsic properties of features and statistical indicators such as fisher score, information gain, chi-square, correlation coefficient. The wrapper method uses a learning algorithm and looks for a subset of features in the feature space that optimize classification accuracy. Therefore, wrapper approaches use meta-heuristic methods for feature subset selection and cross-validation. The hybrid method applies a combination of filter and wrapper methods [2]. Among the feature selection methods, meta-heuristic methods have shown better performance in applications with lots of features [3].

Analyzing extracted features from images and selecting optimal features improves classification performance [4]. In the field of medical imaging, it has been reported many feature selection (FS) studies such as Robustness-Driven FS (RDFS) for lung CT image [5] · Shearlet transform FS from brain MRI image [6] · principal component analysis for lung X-Ray Images [7], genetic algorithm (GA) for lung nodules [8] · bat algorithm (BA) compared with particle swarm optimization (PSO) in lung X-ray images [9], flower pollination algorithm (FPA) from lung images [10].

In the above study, the use of different available methods for classifying patients from lung images by machine vision combined with meta-heuristic algorithms is propounded. On the other, existing diagnostic methods for COVID-19 disease with X-ray images use high memory, long time, and a large number of features. Therefore, the need for an intelligent system seems to be necessary, which helps physicians and treatment staff to classify COVID-

19 patients with high accuracy and high speed to reduce mortality from the disease. The motivation of the research is to plan a smart manner with artificial intelligence methods to aid doctors and patients in COVID-19 prediction and with high accuracy. The novelty of the research is the design of the deep learning structure based feature selection using the binary differential evolution algorithm in COVID-19 diagnosis. The contributions of the study are as:

1- Designing an intelligent system using the deep convolutional neural network without a pre-trained network based on lung X-ray images and extracting features from it with the minimum optimal memory required to create and train the network.

2- Selecting the optimal features of the differential meta-heuristic method that led to the improvement of the performance indexes

3- Increasing the accuracy of classification for multi-class problems, including three categories of patients with COVID-19, pneumonia, and healthy.

The structure of our study is as follows: related works are reviewed in section 2. In section 3, the proposed methodology and model using deep convolution and binary differential algorithm for COVID-19 detections is presented. Experimental results are shown in section 4. Discussion and comparison with other previous works are described in section 5. Finally, the study ends with a conclusion.

## 2. RELATED WORKS

Hemdan, Shouman, & Karar have suggested positive or negative status of COVID with deep learning models [11]. They had reported the VGG19 model was better results with 90% accuracy on 25 COVID, 25 non-COVID images. Toğacıar, Ergen, & Cömert have used 295 COVID, 98 pneumonia, 65 normal images into MobileNet and SqueezeNet [12]. They have extracted features from the models trained Net and then the features were selected by the SMO algorithm. The overall accuracy was 99.27% using the SVM classifier. Zhang, Xie, Li, Shen, & Xia investigated a ResNet model with 18 layers for 100 COVID, 1431 pneumonia images. The value of accuracy was achieved by 95.18% [13]. Apostolopoulos & Mpesiana offered pre-trained VGG19 based on 224 COVID, 700 pneumonia, 504 normal images[14]. The accuracy of their results was 98.75%. In [15] authors considered the DarkNet with 17 convolutional layers using 127 COVID, 500 pneumonia, 500 normal images, and the accuracy was 98.08%. In [16] the performance of CNN was improved using pre-processing image algorithms and the model resulted in 94.5% of accuracy.

In [1] authors designed a COVID-19 classification method which mixed a CNN named Inception pre-trained Imagnet as feature extractor and Marine Predators Algorithm as feature selector, KNN as classifier based on 2 datasets for

two classifications as positive, negative COVID-19 problem. Dataset1 included 200 COVID-19 positive images and 1675 negative also dataset2 contained 219 COVID-19 positive images and 1341 negative images. Accuracy was stated 98.7%, 99.6% for dataset 1, data set2. Canayaz checked a COVID-19 diagnosis model using VGG19, ResNet, AlexNet, and GoogleNet mixed by two meta-heuristic algorithms named binary particle swarm optimization and binary gray wolf optimization. The best overall classification accuracy was 99.38% after feature selection by binary gray wolf optimization based on 1092 X-ray images of COVID-19, pneumonia, and healthy records [17].

One of the limitations of the previous works is the use of pre-trained deep networks that require a lot of memory. In addition, a large number of input features and long detection time are other shortcomings. To improve the detection of COVID-19 by overcoming the above limitations, we proposed the deep learning approach based on feature selection using the binary differential evolution algorithm method.

### 3. METHODOLOGY AND MODEL

The proposed model is shown in Figure 1. First, the lung images enter into the convolutional neural network. After training the network, features are extracted from the images that are not optimal. Optimal features are extracted using the heuristic method. The classification of the three classes named COVID-19, pneumonia, and healthy is done with higher accuracy.

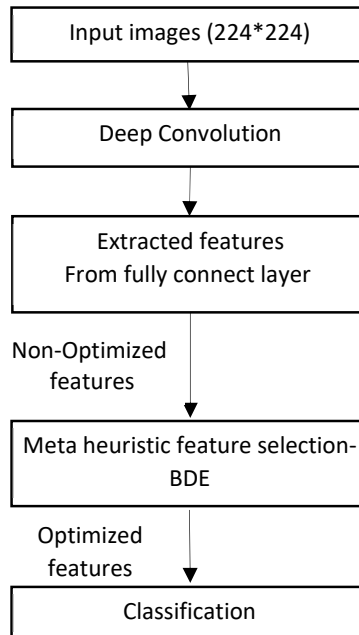


Figure 1. The proposed model for COVID-19

## 2.1. Deep convolution

The convolution neural network is an extractor of features and a suitable classification method in machine learning. In the convolutional network, the input of the network is the original data such as images. The network automatically extracts the features, through the convolution function, after the process of learning, instead of extracting the feature manually. The matrices as the filters, slide on the main input image, and the convolution operation is performed through equation 1. Finally, after training and mapping the input images to the output labels, the features are extracted after several layers of convolution [18].

$$(IMG * C)_{ij} = \sum_{p=0}^{c1-1} \sum_{q=0}^{c2-1} \sum_{c=1}^{tc} C_{p,q,c} \cdot IMG_{i+p,j+q,c} + bs \quad (1)$$

Where IMG is input image with height =H, width =W dimensions, tc is the number of image channels, C is filter matrix with  $c1*c2$  dimensions, bs is a bias value for each filter C,  $i=0\dots H, j=0\dots W$

After applying the convolution, the unwanted values are removed with the ReLu layer and then the input is reduced by the pooling layer. The effective input vector enters the fully connected layer, which has the same function as the MLP. In the final part of the deep convolution layers, Softmax [19], classification layers, performed the classification operation using ADAM (adaptive moment optimizer) [20], bellow lost function (equation 2).

$$L(w, b) = -\frac{1}{M} \sum_{m=1}^M [y_m \log \hat{y}_m + (1 - y_m) \log(1 - \hat{y}_m)] + \Gamma \times \sum_{r=1}^M \|w^r\|_2 \quad (2)$$

Where M is a number of sample images,  $y_m$  is a true class for m-th sample,  $\hat{y}_m$  is predicted output class for m-th input data,  $\Gamma$  is regularization coefficient.

## 2.2. Binary Differential Evolution

Differential evolution (DE) [21] was an evolutionary heuristic method designed for minimizing the continuous problem. Binary differential evolution (BDE) [22] expanded for feature selection issue. It has three main builders named mutation, crossover, and selection. First, the initial population is produced by dimensions D, which D is the number of features that we want to optimize. For the mutation operation, three random vectors  $p_{u1}, p_{u2}, p_{u3}$  are selected for vector  $p_k$  such that  $u1 \neq u2 \neq u3 \neq k$ , k is a vector arrangement in population

If d-th dimension of a vector  $p_{u1}$  and vector  $p_{u2}$  be equal, the d-th feature of the difference vector (equation 3) will be zero, otherwise, it takes the same value as a vector  $p_{u1}$ .

$$difference\ vector_k^d = \begin{cases} 0 & p_{u1}^d = p_{u2}^d \\ p_{u1} & other \end{cases} \quad (3)$$

Afterward, the mutation and crossover are executed as shown in equations 4 and 5.

$$mute\ vector_k^d = \begin{cases} 1, & if\ difference\ vector_k^d = 1 \\ p_{u3}^d, & other \end{cases} \quad (4)$$

$$W_k^d = \begin{cases} \text{muted vector}_k^d, & \text{if } \gamma \leq CR \text{ || } d = d_{\text{random}} \\ p_k^d, & \text{other} \end{cases} \quad (5)$$

Where  $W$  is the try vector,  $CR \in (0, 1)$  is crossover amount,  $\gamma \in (0, 1)$  is a random number. In the selection procedure, if the fitness value of the try vector  $W_k$  be better than the current vector  $p_k$  will replace it. Otherwise, the current vector  $p_k$  is stored for the next generation.

#### 4. EXPERIMENTAL RESULTS

##### 4.1. Description of data

Canayaz created a COVID-19 X-ray data set including three classes of patients with COVID-19, pneumonia, and healthy [17]. In this database, there are 364 images for each of the three categories that is obtained as a balanced dataset by combining data [23-25]. The total number of images are equal to the number of classes multiplied by the number of class instances, hence  $(3*394)1092$  and its dimensions are  $224 \times 224$ . In this study, the same data are used to predict COVID-19 disease with the convolutional neural network and select optimal features by the meta-heuristic algorithm named binary differential. Figure 2 shows one sample of three output classes as COVID-19, pneumonia, and healthy.



Figure 2. The Chest X-ray images of different conditions (a) COVID-19 (b) Pneumonia (c) Healthy

##### 4.2. Performance evaluation

The suggested model was performed in Matlab version 9.1.0.441655 (R2018b) on a notebook PC with, 1.8 GHz CPU, and 4 Gigabyte RAM. The proposed method takes an average of 29 seconds per patient after training in the application phase, which can be reduced by improving the hardware technology used[۲۴ ,۲۵] . The Accuracy, sensitivity, specificity, geometric mean, and area under curve (AUC-ROC)[28, 29] as performance evaluation metrics (equations 6-9) were considered to measure the COVID 19 prediction model. The correctness of classification is named accuracy. The amount of the negatives that are correctly distinguished is specificity, the amount of the positives that are correctly distinguished is sensitivity. The second root of the product of sensitivity, specificity is called the geometric mean. Higher values of the area under the curve (AUC) in the receiver operating characteristics indicate better classification performance.

$$Accuracy = \frac{TP+TN}{TP+TN+FP+FN} \quad (6)$$

Where:

True positives = the number of samples that are correctly labelled as positive

False positives = the number of samples that are wrongly labelled as positive

True negatives = the number of samples that are correctly labelled as negative

False negatives = the number of samples that are wrongly labelled as negative

$$\text{Sensitivity} = TP / (TP+ FN) \quad (7)$$

$$\text{Specificity} = TN / (FP+TN) \quad (8)$$

$$\text{Geometric mean} = \sqrt[2]{\text{Sensitivity} * \text{Specificity}} \quad (9)$$

#### 4.3. Model parameters

The structure of the deep convolution neural network is shown in Figure 3. Firstly, the dimensions of images in the image input layer were 224\*224, there were 8 filters 3-by-3 for convolution operator. The local features automatically are extracted after processing the first block of the network layers, ie image input, convolution, Batch Normalize, ReLU, max-pooling layers, fully connected layer 400, ReLU, Drop out. Finally, the second network block, including three- fully connected layers, softmax, classification categorizes the input images into three output classes. The validation accuracy after 200 epochs was 97.25% using ADAM optimizer during training and the mini-batch size was 64 (Figure 4). The batch normalization and dropout are put due to regularize neural network and barricade overfitting.

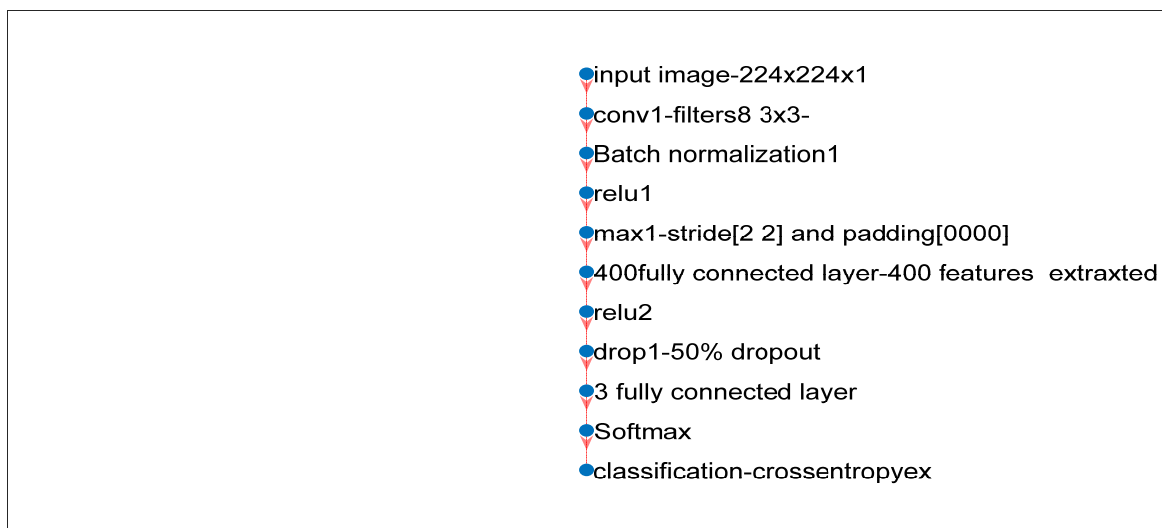


Figure. 3. Structure of proposed model layers

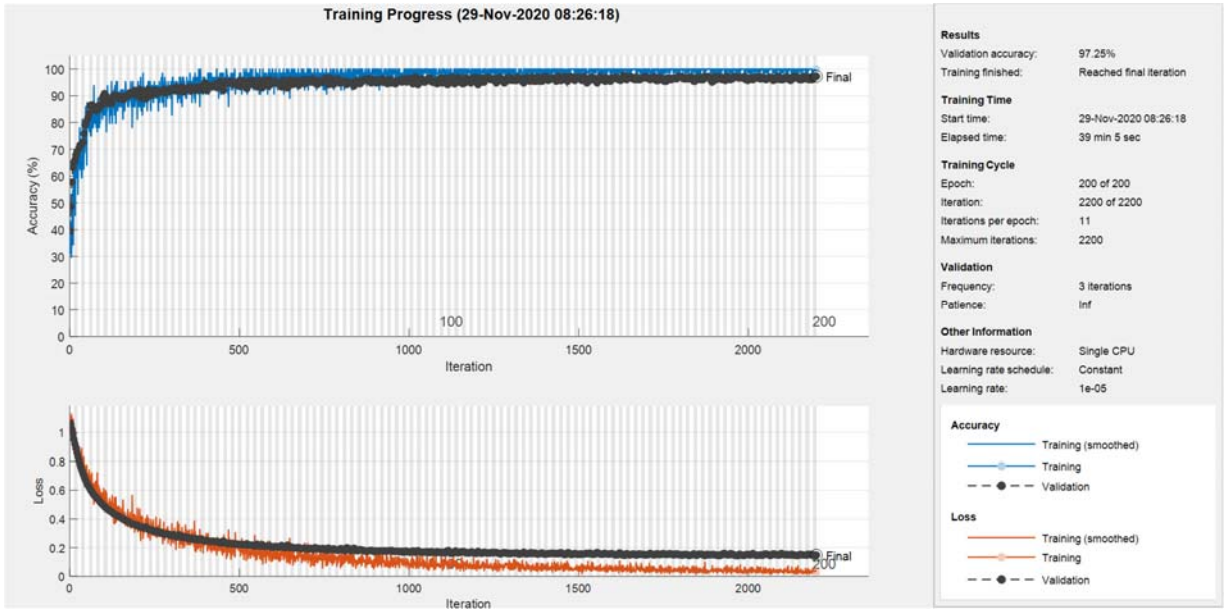


Figure 4. Accuracy and loss measure for training, validation data using convolution neural networks

Convolution networks are a method for converting the input to feature vectors. Since some network features may cause poor performance of the model [1], therefore after extracting 400 features in the first fully Connect layer, the meta-heuristic algorithm named binary differential was used to select the optimal features subset and remove the useless features. In the binary differential algorithm, population = 20, iteration= 100 (figure 5), and a crossover rate of 1 were the parameters of the algorithm. Amount (1- (geometric mean)) of the SVM classifier [30] was considered as fitness values of the population (Figure 5). After executing the binary differential algorithm, 340 optimal features were selected.

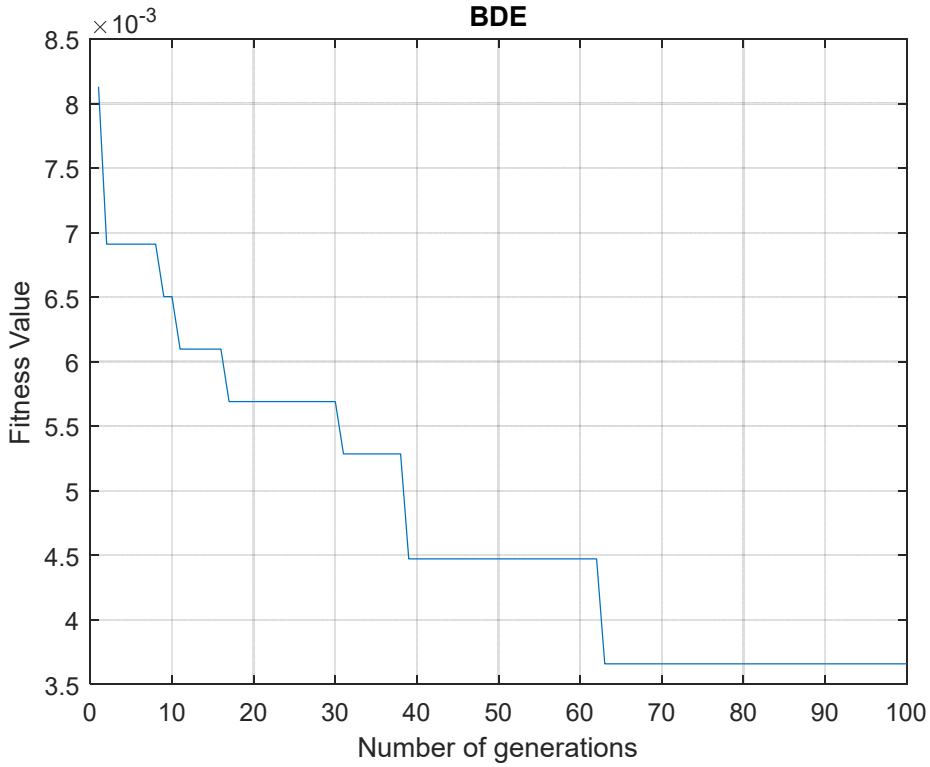


Figure 5. Fitness curve for the Binary differential algorithm

#### 4.4. Performance comparison

Of the total data, 70% of the data was considered for the train, 15% for the validation, and 15% for the test. To prevent overfitting, the proposed method was applied to the data 100 runs [31]. Both the optimal selected features by the differential algorithm and the initial extracted features from the deep convolution neural network entered into the SVM classifier.

Table 1 demonstrated the confusion matrix using train, test, validation, and total data for original features and optimized features are applied by SVM classifier. The tp, tn, fp, fn, accuracy, sensitivity, specificity, geometric mean, AUC metrics for each of the three output classes, and each type of test, train, validation, and total data were computed (Table2).

## 5. DISCUSSION

Applying images to a deep neural network can be used to predict disease. In other words, a deep neural network can be exerted as a feature extractor. The large size and high volume of images applied to the deep neural network produced many features that prolonged the training time and decision time of the predictive model.

The design challenges of the proposed model were: first: collect lung images and improve them. Secondly, deep network architecture, including structure, number, and type of layers. Third, the type of meta-heuristic algorithm, the initial population, and the objective function type of the meta-heuristic algorithm. The presence of inefficient features extracted from the deep network could reduce the accuracy and efficiency of the predictive model. Therefore, selecting the optimal features by the meta-heuristic method improved the memory, time, and accuracy of the model.

According to Table 3, the proposed model based on the extracted features from X-ray image using CNN and selected optimized features by the binary differential meta-heuristic algorithm has attained an accuracy of 99.43%, a sensitivity of 99.16%, a specificity of 99.57%, a gmean of 99.37%, AUC of 0.99, and a root mean square error (RMSE) of 0.1133. In this paper accuracy for the classification of the COVID -19 issue was calculated to be 99.43%, and the count of relevant features was 304 (Table 4) whereas in the previous study [17] based on the same data they were reported to be 99.38%, 448 features.

For future work, using another feature selection algorithm and applying other learners may yield better results. In addition to the images, the parameters derived from the clinical trials can create a new model with a new combination of features to diagnose the disease or possibly predict its death. In addition to the images, the parameters extracted from the clinical trials can create a new model with a new combination of features, which may be effective in diagnosing the disease or possibly predicting its death.

Table 1. Average of a confusion matrix for 100 runs with 3 classes by the (a) optimized features (b) original features based on train, test, validation, and total data

(a) Optimized features

Optimized features test		Predicted		
		Covid	Normal	Pneumonia
actual	Covid	51/75	0	0/2
	Normal	0/15	54/9	0/1
	Pneumonia	0/4	0/55	55/95

(b) Original features

Original features test		Predicted		
		Covid	Normal	Pneumonia
Actual	Covid	51/65	0	0/3
	Normal	0/25	54/65	0/25
	Pneumonia	0/5	0/95	55/45

Optimized features validation		Predicted		
		Covid	Normal	Pneumonia
actual	Covid	55/05	0/05	0/45
	Normal	0/05	54/4	0/3
	Pneumonia	0/4	1	52/3

original features validation		Predicted		
		Covid	Normal	Pneumonia
actual	Covid	54/85	0	0/7
	Normal	0/15	54/2	0/4
	Pneumonia	0/55	1/2	51/95

Optimized features train		Predicted		
		Covid	Normal	Pneumonia
actual	Covid	256/5	0	0
	Normal	0	254/1	0
	Pneumonia	0	0	253/4

Original features train		Predicted		
		Covid	Normal	Pneumonia
Actual	Covid	256/45	0	0/05
	Normal	0	254/1	0
	Pneumonia	0	0	253/4

Optimized features total		Predicted		
		Covid	Normal	Pneumonia
Actual	Covid	363/3	0/05	0/65
	Normal	0/2	363/4	0/4
	Pneumonia	0/8	1/55	361/65

original features total		Predicted		
		Covid	Normal	Pneumonia
actual	Covid	362/95	0	1/05
	Normal	0/4	362/95	0/65
	Pneumonia	1/05	2/15	360/8

Table 2. Comparison of indicators (TP, TN, FP, FN, accuracy, the area under curve, sensitivity, specificity, geometric mean) for any output class based on (a) optimized features (b) original features

(a) Optimized features				(b) Original features			
Optimized features -total	Covid	Normal	Pneumonia	Original features -total	Covid	Normal	Pneumonia
TP	363/30	363/40	361/65	TP	362/95	362/95	360/80
TN	727/00	726/40	726/95	TN	726/55	725/85	726/30
FP	1/00	1/60	1/05	FP	1/45	2/15	1/70
FN	0/70	0/60	2/35	FN	1/05	1/05	3/20
Accuracy	99/84	99/80	99/69	Accuracy	99/77	99/71	99/55
Sensitivity	99/81	99/84	99/35	Sensitivity	99/71	99/71	99/12
Specificity	99/86	99/78	99/86	Specificity	99/80	99/70	99/77
geometric mean	99/84	99/81	99/60	geometric mean	99/76	99/71	99/44
area under curve	0/9984	0/9981	0/9961	area under curve	0/9976	0/9971	0/9944
Optimized features -train	Covid	Normal	pneumonia	Original features -train	Covid	Normal	pneumonia
TP	256/50	254/10	253/40	TP	256/45	254/10	253/40
TN	507/50	509/90	510/60	TN	507/50	509/90	510/55
FP	0/00	0/00	0/00	FP	0/00	0/00	0/05
FN	0/00	0/00	0/00	FN	0/05	0/00	0/00
Accuracy	100/00	100/00	100/00	Accuracy	99/99	100/00	99/99
Sensitivity	100/00	100/00	100/00	Sensitivity	99/98	100/00	100/00
Specificity	100/00	100/00	100/00	Specificity	100/00	100/00	99/99
geometric mean	100/00	100/00	100/00	geometric mean	99/99	100/00	100/00
area under curve	1/0000	1/0000	1/0000	area under curve	0/9999	1/0000	1/0000
Optimized features -test	Covid	Normal	Pneumonia	Original features -test	Covid	Normal	Pneumonia
TP	51/75	54/90	55/95	TP	51/65	54/65	55/45
TN	111/50	108/30	106/80	TN	111/30	107/90	106/55
FP	0/55	0/55	0/30	FP	0/75	0/95	0/55
FN	0/20	0/25	0/95	FN	0/30	0/50	1/45
Accuracy	99/54	99/51	99/24	Accuracy	99/36	99/12	98/78
Sensitivity	99/62	99/55	98/33	Sensitivity	99/42	99/09	97/45
Specificity	99/51	99/49	99/72	Specificity	99/33	99/13	99/49
geometric mean	99/56	99/52	99/02	geometric mean	99/38	99/11	98/46
area under curve	0/9956	0/9952	0/9903	area under curve	0/9937	0/9910	0/9847
Optimized features -valid	Covid	Normal	Pneumonia	Original features -valid	Covid	Normal	Pneumonia
TP	55/05	54/40	52/30	TP	54/85	54/20	51/95
TN	108/00	108/20	109/55	TN	107/75	108/05	109/20
FP	0/45	1/05	0/75	FP	0/70	1/20	1/10
FN	0/50	0/35	1/40	FN	0/70	0/55	1/75
Accuracy	99/42	99/15	98/69	Accuracy	99/15	98/93	98/26
Sensitivity	99/10	99/36	97/39	Sensitivity	98/74	99/00	96/74
Specificity	99/59	99/04	99/32	Specificity	99/35	98/90	99/00
geometric mean	99/34	99/20	98/35	geometric mean	99/05	98/95	97/87
area under curve	0/9934	0/9920	0/9840	area under curve	0/9904	0/9895	0/9789

Table 3. Average of confusion matrix components for 100 runs by the original features and optimized features

Method	TP	TN	FP	FN	Accuracy	Sensitivity	Specificity	Geometric mean	Area Under Curve	RMSE
Original features by Deep convolution										
Training	254/65	509/32	0/02	0/02	1/0000	0/9999	1/0000	1/0000	0/9999	0/0036
Testing	53/92	108/58	0/75	0/75	0/9909	0/9866	0/9931	0/9898	0/9898	0/1533
Validation	53/67	108/33	1/00	1/00	0/9878	0/9816	0/9909	0/9862	0/9863	0/1905
Total	362/23	726/23	1/77	1/77	0/9968	0/9951	0/9976	0/9964	0/9964	1/1543
Optimized features by Binary Differential										
Training	254/67	509/33	0/00	0/00	1/0000	1/0000	1/0000	1/0000	1/0000	0/0000
Testing	54/20	108/87	0/47	0/47	0/9943	0/9916	0/9957	0/9937	0/9937	0/1133
Validation	53/92	108/58	0/75	0/75	0/9909	0/9862	0/9931	0/9896	0/9898	0/1592
Total	362/78	726/78	1/22	1/22	0/9978	0/9967	0/9983	0/9975	0/9975	1/1543

Table 4. Comparison of the suggested approach with related prior research

research	Method	Number of features	Accuracy	Geometric mean	RAM	Max Computation time
[17]	Binary particle swarm optimization -VGG19	448	99.38	-	16 gigabyte	2500s
Proposed method	Binary differential -cnn	308	99.43	99.37	4 gigabyte	2300s

## 6. CONCLUSION

The number of people with COVID-19 disease has rapidly expanded. The usage of machine vision techniques and artificial intelligence as an aid plays an important role in diagnosing the disease and helping to treat it. The purpose of this paper was to develop a method for problem COVID-19. A data set of lung images, including three categories of pneumonia, COVID-19, healthy were considered.

A deep convolution neural network consisting of 11 layers was applied to extract the features. Relevant features were selected by the binary differential meta-heuristic method and unrelated features were removed. Lung X-ray images were classified based on these optimal features using a SVM classifier. The results of this study showed that the accuracy indicator, the number of relevant extracted features had better performance on the same data than previous methods. The proposed model based on a deep neural network and meta-heuristic algorithm for feature selection can be used in other medical applications.

## Summary points

### What was Already Known on the topic?

- chest X-ray is an imaging approach to detect COVID-19.
- Deep learning method-based X-ray with pre-train network use in features extraction of images for prediction of COVID-19.
- More researches reported two classification problems as COVID-19, and healthy.

### What this study adds to our knowledge

- using the deep convolutional neural network without a pre-trained network based on chest X-ray images and extracting features from it can optimize the needed memory.
- Deep learning mixed meta-heuristic technique (binary differential algorithm) can enhance feature selection and improve model performance.
- Increasing the accuracy of classification for multi-class problems, including three categories of patients with COVID-19, pneumonia, and healthy can achieve.

## Authors' contributions

Iraji and Feizi-Derakshhi suggested the algorithm for image analysis; iraji implemented it and analyzed the experimental results; Tanha provided clinical guidance; Iraji, Feizi-Derakhshi, and Tanha consulted the obtained result. All authors read and approved the final manuscript.

## Funding

This research received no specific grant from any funding agency in the public, commercial, or not-for-profit sectors.

## Availability of data and materials

The datasets used and analyzed during the current study are available from the corresponding author on reasonable request.

## DISCLOSURE OF POTENTIAL CONFLICTS OF INTEREST

### Conflicts of interest

The authors declared no potential conflicts of interest with respect to the research, authorship, and/or publication of this article.

### Ethical approval

This article does not contain any data, or other information from studies or experimentation, with the involvement of human or animal subjects.

### Consent for publication

Agreed by the authors.

### Competing interests

The authors declare that they have no competing interests.

## REFERENCES

- 1       Sahlol, A.T., Yousri, D., Ewees, A.A., Al-Qaness, M.A., Damasevicius, R., and Abd Elaziz, M.: 'COVID-19 image classification using deep features and fractional-order marine predators algorithm', *Scientific Reports*, 2020, 10, (1), pp. 1-15
- 2       Hoque, N., Bhattacharyya, D.K., and Kalita, J.K.: 'MIFS-ND: A mutual information-based feature selection method', *Expert Systems with Applications*, 2014, 41, (14), pp. 6371-6385
- 3       Dey, N.: 'Advancements in applied metaheuristic computing' (IGI Global, 2017. 2017)
- 4       Lambin, P., Rios-Velazquez, E., Leijenaar, R., Carvalho, S., Van Stiphout, R.G., Granton, P., Zegers, C.M., Gillies, R., Boellard, R., and Dekker, A.: 'Radiomics: extracting more information from medical images using advanced feature analysis', *European journal of cancer*, 2012, 48, (4), pp. 441-446
- 5       Chong, D.Y., Kim, H.J., Lo, P., Young, S., McNitt-Gray, M.F., Abtin, F., Goldin, J.G., and Brown, M.S.: 'Robustness-driven feature selection in classification of fibrotic interstitial lung disease patterns in computed tomography using 3D texture features', *IEEE transactions on medical imaging*, 2015, 35, (1), pp. 144-157
- 6       Acharya, U.R., Fernandes, S.L., WeiKoh, J.E., Ciaccio, E.J., Fabell, M.K.M., Tanik, U.J., Rajinikanth, V., and Yeong, C.H.: 'Automated detection of Alzheimer's disease using brain MRI images—a study with various feature extraction techniques', *Journal of Medical Systems*, 2019, 43, (9), pp. 302
- 7       Afzali, A., Mofrad, F.B., and Pouladian, M.: 'Feature Selection for Contour-based Tuberculosis Detection from Chest X-Ray Images', in Editor (Ed.)^(Eds.): 'Book Feature Selection for Contour-based Tuberculosis Detection from Chest X-Ray Images' (IEEE, 2019, edn.), pp. 194-198

8 Da Silva, S.F., Ribeiro, M.X., Neto, J.d.E.B., Traina-Jr, C., and Traina, A.J.: 'Improving the ranking quality of medical image retrieval using a genetic feature selection method', *Decision support systems*, 2011, 51, (4), pp. 810-820

9 Li, J., Fong, S., Liu, L.-s., Dey, N., Ashour, A.S., and Moraru, L.: 'Dual feature selection and rebalancing strategy using metaheuristic optimization algorithms in X-ray image datasets', *Multimedia Tools and Applications*, 2019, 78, (15), pp. 20913-20933

10 Johnson, D.S., Johnson, D.L.L., Elavarasan, P., and Karunanithi, A.: 'Feature Selection Using Flower Pollination Optimization to Diagnose Lung Cancer from CT Images', in Editor (Ed.)^(Eds.): 'Book Feature Selection Using Flower Pollination Optimization to Diagnose Lung Cancer from CT Images' (Springer, 2020, edn.), pp. 604-620

11 Hemdan, E.E.-D., Shouman, M.A., and Karar, M.E.: 'Covidx-net: A framework of deep learning classifiers to diagnose covid-19 in x-ray images', *arXiv preprint arXiv:2003.11055*, 2020

12 Toğacar, M., Ergen, B., and Cömert, Z.: 'COVID-19 detection using deep learning models to exploit Social Mimic Optimization and structured chest X-ray images using fuzzy color and stacking approaches', *Computers in Biology and Medicine*, 2020, pp. 103805

13 Zhang, J., Xie, Y., Li, Y., Shen, C., and Xia, Y.: 'Covid-19 screening on chest x-ray images using deep learning based anomaly detection', *arXiv preprint arXiv:2003.12338*, 2020

14 Apostolopoulos, I.D., and Mpesiana, T.A.: 'Covid-19: automatic detection from x-ray images utilizing transfer learning with convolutional neural networks', *Physical and Engineering Sciences in Medicine*, 2020, pp. 1

15 Ozturk, T., Talo, M., Yildirim, E.A., Baloglu, U.B., Yildirim, O., and Acharya, U.R.: 'Automated detection of COVID-19 cases using deep neural networks with X-ray images', *Computers in Biology and Medicine*, 2020, pp. 103792

16 Heidari, M., Mirniaharikandehei, S., Khuzani, A.Z., Danala, G., Qiu, Y., and Zheng, B.: 'Improving the performance of CNN to predict the likelihood of COVID-19 using chest X-ray images with preprocessing algorithms', *International journal of medical informatics*, 2020, 144, pp. 104284

17 Canayaz, M.: 'MH-COVIDNet: Diagnosis of COVID-19 using deep neural networks and metaheuristic-based feature selection on X-ray images', *Biomedical Signal Processing and Control*, 2020, 64, pp. 102257

18 Gao, Y., Zhu, T., and Xu, X.: 'Bone age assessment based on deep convolution neural network incorporated with segmentation', *International Journal of Computer Assisted Radiology and Surgery*, 2020, 15, (12), pp. 1951-1962

19 Adem, K., Kılıçarslan, S., and Cömert, O.: 'Classification and diagnosis of cervical cancer with stacked autoencoder and softmax classification', *Expert Systems with Applications*, 2019, 115, pp. 557-564

20 Khaire, U.M., and Dhanalakshmi, R.: 'High-dimensional microarray dataset classification using an improved adam optimizer (iAdam)', *Journal of Ambient Intelligence and Humanized Computing*, 2020, 11, (11), pp. 5187-5204

21 Storn, R., and Price, K.: 'Differential evolution—a simple and efficient heuristic for global optimization over continuous spaces', *Journal of global optimization*, 1997, 11, (4), pp. 341-359

22 Zorarpaci, E., and Özel, S.A.: 'A hybrid approach of differential evolution and artificial bee colony for feature selection', *Expert Systems with Applications*, 2016, 62, pp. 91-103

23 Cohen, J.P., Morrison, P., Dao, L., Roth, K., Duong, T.Q., and Ghassemi, M.: 'Covid-19 image data collection: Prospective predictions are the future', *arXiv preprint arXiv:2006.11988*, 2020

24 Chowdhury, M.E., Rahman, T., Khandakar, A., Mazhar, R., Kadir, M.A., Mahbub, Z.B., Islam, K.R., Khan, M.S., Iqbal, A., and Al-Emadi, N.: 'Can AI help in screening viral and COVID-19 pneumonia?', *arXiv preprint arXiv:2003.13145*, 2020

25 Kermany, D., Zhang, K., and Goldbaum, M.: 'Labeled optical coherence tomography (OCT) and Chest X-Ray images for classification', *Mendeley data*, 2018, 2

26 Rajinikanth, V., Dey, N., Raj, A.N.J., Hassanien, A.E., Santosh, K., and Raja, N.: 'Harmony-search and otsu based system for coronavirus disease (COVID-19) detection using lung CT scan images', arXiv preprint arXiv:2004.03431, 2020

27 Dey, N., Rajinikanth, V., Fong, S.J., Kaiser, M.S., and Mahmud, M.: 'Social group optimization-assisted Kapur's entropy and morphological segmentation for automated detection of COVID-19 infection from computed tomography images', Cognitive Computation, 2020, 12, (5), pp. 1011-1023

28 Farag, A.A., Ali, A., Elshazly, S., and Farag, A.A.: 'Feature fusion for lung nodule classification', International journal of computer assisted radiology and surgery, 2017, 12, (10), pp. 1809-1818

29 Li, Z., Jiang, J., Zhou, H., Zheng, Q., Liu, X., Chen, K., Weng, H., and Chen, W.: 'Development of a deep learning-based image eligibility verification system for detecting and filtering out ineligible fundus images: A multicentre study', International Journal of Medical Informatics, 2021, 147, pp. 104363

30 Xu, L., Wang, X., Bai, L., Xiao, J., Liu, Q., Chen, E., Jiang, X., and Luo, B.: 'Probabilistic SVM classifier ensemble selection based on GMDH-type neural network', Pattern Recognition, 2020, 106, pp. 107373

31 Kuncheva, L.I.: 'Combining pattern classifiers: methods and algorithms' (John Wiley & Sons, 2014. 2014)